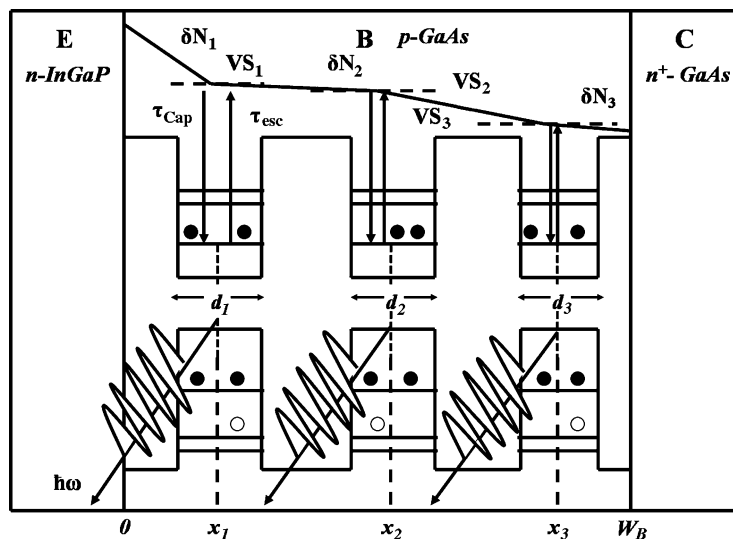


Modeling Resonance-Free Modulation Response in Transistor Lasers With Single and Multiple Quantum Wells in the Base

Volume 4, Number 5, October 2012

Rikmantra Basu, Member, IEEE
Bratati Mukhopadhyay, Member, IEEE
P. K. Basu, Senior Member, IEEE



DOI: 10.1109/JPHOT.2012.2211075
1943-0655/\$31.00 ©2012 IEEE

Modeling Resonance-Free Modulation Response in Transistor Lasers With Single and Multiple Quantum Wells in the Base

Rikmantra Basu,^{1,2} *Member, IEEE*, Bratati Mukhopadhyay,¹ *Member, IEEE*,
and P. K. Basu,¹ *Senior Member, IEEE*

¹Institute of Radio Physics and Electronics, University of Calcutta, Kolkata 700 009, India

²Centre for Research in Nanoscience and Nanotechnology, University of Calcutta,
Kolkata 700 106, India

DOI: 10.1109/JPHOT.2012.2211075
1943-0655/\$31.00 ©2012 IEEE

Manuscript received July 8, 2012; revised July 24, 2012; accepted July 24, 2012. Date of publication August 10, 2012; date of current version August 17, 2012. The work of R. Basu was supported by the Council of Scientific and Industrial Research (CSIR), Govt. of India through a Senior Research Fellowship (No. 09/028(0861)/2012-EMR-I). The work of P. K. Basu was supported by the University Grants Commission India through a UGC-BSR Faculty Fellowship. Corresponding author: R. Basu (e-mail: rikmantra@gmail.com).

Abstract: We have developed the expressions for terminal currents in transistor lasers (TLs) having a single quantum well (SQW) as well as multiple quantum wells (MQWs) of different well and barrier widths in the base by solving a continuity equation relating the bulk carrier density with the 2-D carrier density via virtual states (VS). The gain in the quantum well (QW) is obtained by considering strain, 2-D density-of-states, polarization-dependent momentum matrix element, Fermi statistics, and Lorentzian broadening. A calculated value of 7.06 mA of threshold base current for three 16-nm-wide QWs in the base indicates a substantial reduction from the calculated and experimental value of 21.5 mA for a 16-nm-wide InGaAs QW in GaAs base. A similar reduction is also obtained for three QWs of different widths having variable barrier widths. The estimated modulation bandwidths (BWs) are higher in the case of MQW structures than in the SQW TL. Above threshold, the effective base recombination time, including spontaneous and stimulated processes, gives rise to a fast recombination process in the base, which leads to resonance-free modulation response. The estimated recombination time compares favorably with the value reported from the analysis of experimental data.

Index Terms: Transistor laser, semiconductor laser, heterojunction bipolar transistor, small-signal modulation, resonance-free modulation.

1. Introduction

The transistor laser (TL), invented by Feng, Holonyak and coworkers [1], [2], contains a quantum well (QW) incorporated in the base of a heterojunction bipolar transistor (HBT). When the carriers injected into the base under a forward bias applied to the emitter–base (EB) junction are sufficient in number to create population inversion between the conduction and the valence subbands of the QW, and to make the optical gain overcome the material and mirror losses, laser emission emerges in a direction normal to the current flow in the transistor.

Since its announcement, almost all the experimental reports about the TL appearing in the literature have come from the group led by Feng and Holonyak [3]–[7]. The group also presented some analytical models to predict or explain the current–voltage and light–current characteristics and the modulation bandwidth (BW) [4]–[7]. A circuit model has also been developed by the

group [7]. Analytical and numerical models for terminal currents, modulation BW, etc., of TLs are also developed by few other groups [8]–[10]. The features of these models have been briefly discussed in a recent paper by Basu *et al.* [10], in which a more general analytical model is proposed. The values of threshold base current, light power output, and the charge carrier distribution profile, obtained in that work [10], agree satisfactorily with the experimental results reported by Feng and his coworkers [3]–[7].

In all the experimental and theoretical studies mentioned above, the active region is a QW embedded in the base of an HBT. It is well known that the performance of a laser is improved, especially in reducing the threshold current, if a single QW (SQW) is replaced by multiple QWs (MQWs), primarily because the mode confinement is enhanced in the latter [11]. The increase in the modulation BW in an MQW TL has been predicted in a recent paper [12].

In the present paper, we make an attempt to formulate a general and complete analytical model of a TL with MQWs in the base region and to ascertain to what extent the threshold current and modulation BW of an MQW TL improve with respect to an SQW TL. In addition, we also estimate the values of recombination time that eliminates the presence of a resonance peak in the small-signal modulation response. This peak in a laser diode poses problems in high-bit-rate data communication and limits the number of channels to be used. The peak can be removed by inserting a Bessel filter, which no doubt increases the complexity in the circuit. Feng *et al.* [6] proposed that a tilted base charge distribution in a diode or present in a TL may eliminate the resonance peak and enhance the modulation BW. In their analysis, the authors have taken the efficiency and differential gain constant as a constant fitting parameter. In our present work, these quantities have been estimated from first principles.

In this context, it may be mentioned that theoretical works on modulation response for an SQW TL have been presented by a number of groups [4]–[6], [8], [9], [12]–[14]. While the analysis in [4] and [6] and in [8] and [13] are analytical, the results obtained in [9], [12], and [14] are based on numerical solution of coupled rate equations. Faraji *et al.* [8], [13] showed that a larger BW may be obtained in an SQW TL than in QW diode lasers. Shirao *et al.* [14] showed that ringing-free optical pulse might result in response to a square electrical pulse when the recombination time is reduced substantially. In the recent report by Taghavi *et al.* [12], the modulation BW has been optimized, taking into consideration a number of QWs. None of these papers, however, made any attempt to compare the calculated values with the experimental values, which exist at least for SQW TLs.

In our present work, both symmetric and asymmetric MQWs are considered, and the threshold currents are compared with the previously reported value [10] for the TL with an SQW in the base region. We then develop the simple theory for optical response for a TL with MQWs in the base and compare the values of modulation BW with the existing results for an SQW TL. Reduction in the threshold base current and also an increase in modulation BWs for this symmetric MQW (S-MQW) TL are observed. Similar calculations are repeated for different widths of QWs and barriers (asymmetric MQW: A-MQW) TL. The effective recombination lifetime, including spontaneous and stimulated processes, leading to resonance-free modulation response is then estimated and compared with the reported values [6].

The modulation response of QW laser diodes is an extensively studied subject, both theoretically and experimentally. Previously, the relation of various carrier processes (i.e., carrier recombination, carrier escape, and carrier capture) on the threshold current [15] and frequency modulation [16], [17] characteristics in QW diode lasers had been reported. Suppressing the thermionic carrier escape rates in QW lasers [18] had been shown to improve the current injection efficiency in QW lasers [15], which, in turn, leads to reduction in carrier leakages and threshold current in QW lasers [19], [20]. In addition, the improved suppression of thermionic carrier escape in QW are important for improving the high-temperature frequency modulation characteristic in QW lasers [21], [22] as well as suppressing the efficiency-droop in QW light-emitting diodes [23], [24]. Thus, our current studies to provide improved understanding in the relation of various carrier processes to the threshold and frequency modulation properties in QW-based TLs are important for optimizing the laser characteristics.

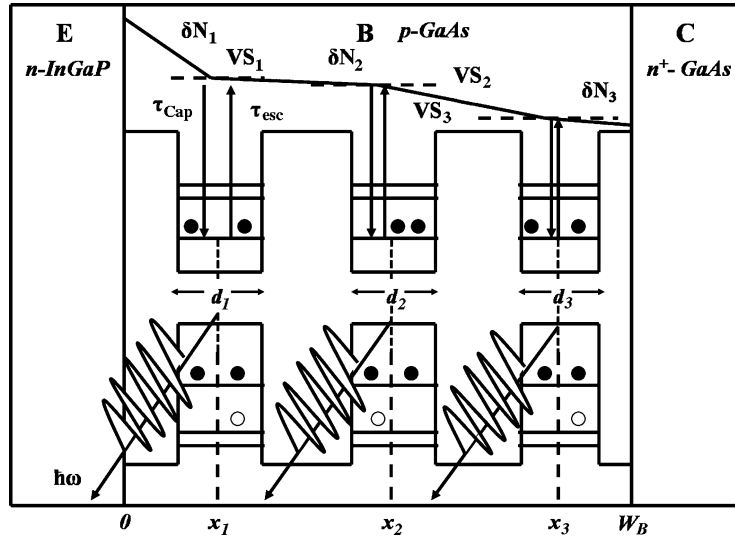


Fig. 1. Schematic diagram of MQW TL structure, showing band diagram, charge distribution profile, and some intrinsic processes.

The analytical model is presented in Section 2, and the calculated results are given in Section 3, in which comparisons with previous data are made. Section 4 concludes our work.

2. Theory

The SQW TL structure considered is the usual HBT with higher band gap *N*-type InGaP emitter (E) layer, *p*-type GaAs base (B) layer with an InGaAs QW embedded in it, and an *n*-type GaAs collector (C) layer [10] with an effective area of $4000 \mu\text{m}^2$. The InGaAs SQW of width 16 nm is assumed to be placed at 59 nm in GaAs base of width $W_B = 88$ nm, corresponding to the structure used in experiments. The S-MQW TL considered in this work consists of three QWs of equal widths of 16 nm and similar barrier width of 20 nm with the middle QW placed at 59 nm. Different QW widths of 12, 16, and 18 nm, respectively, are considered in case of an A-MQW TL structure, where the middle QW is also placed at 59 nm away from the EB junction. The simplified band diagram and charge density profile including other basic intrinsic processes for MQW structure are shown in Fig. 1 schematically. In the diagram, $x = 0$ is the position of the EB junction; W_B is the base width; and x_1 , x_2 , and x_3 are the coordinates of the center of the three QWs, respectively. The finite widths d_1 , d_2 , and d_3 of the QWs are neglected in our analysis for terminal currents.

We assume that the transport of minority carriers in the base is solely limited by diffusion process as justified in our earlier work [10]. The solution of time-independent continuity equation for diffusion-dominated transport before the n th QW located at position x_n leads to the following for the carrier concentration

$$\delta N_n^-(x) = \left[\frac{N_{VS_n} e^{-x_{n-1}/L_D} - (J_{VS})_{n-1} e^{-x_{n-1}/L_D}}{2 \cosh\left(\frac{x_n - x_{n-1}}{L_D}\right)} \right] e^{x/L_D} + \left[\frac{N_{VS_1} e^{x_{n-1}/L_D} + (J_{VS})_{n-1} e^{x_{n-1}/L_D}}{2 \cosh\left(\frac{x_n - x_{n-1}}{L_D}\right)} \right] e^{-x/L_D} \quad (1)$$

where J_{VS} and N_{VS} are, respectively, the current density and the electron density related to the virtual states (VS).

Similarly, carrier concentration after the n th QW becomes

$$\delta N_n^+(x) = \left[\frac{-N_{VS_n} e^{-W_B/L_D}}{2 \sinh\left(\frac{W_B - x_n}{L_D}\right)} \right] e^{x/L_D} + \left[\frac{N_{VS_n} e^{W_B/L_D}}{2 \sinh\left(\frac{W_B - x_n}{L_D}\right)} \right] e^{-x/L_D}. \quad (2)$$

Thus, having any arbitrary number, n , of QWs in an MQW structure, the generalized expression for the emitter current expression becomes

$$J_E = \frac{qD_n}{L_D} \left[\sum_{i=1}^n \left\{ (N_{VS})_i \left[\tanh\left(\frac{x_i - x_{i-1}}{L_D}\right) - \coth\left(\frac{x_i - x_{i-1}}{L_D}\right) \right] + \frac{(N_{VS})_{i+1}}{\sinh\left(\frac{x_i - x_{i-1}}{L_D}\right)} - \frac{(J_{VS})_i \cdot L_D}{q \cdot D_n} \right\} \times \prod_{m=1}^i \cosh\left(\frac{x_m - x_{m-1}}{L_D}\right) \right]. \quad (3)$$

By similar fashion, the collector current is expressed as

$$\begin{aligned} J_C = & \sum_{i=1}^n \left[\frac{J_E q D_n \cosh\left(\frac{W_B - x_i}{L_D}\right)}{L_D \cosh\left(\frac{x_i}{L_D}\right) \cosh\left(\frac{x_{i+1} - x_i}{L_D}\right)} \right] \\ & - \sum_{i=1}^n \left[\frac{N_{VS_i} q D_n \cosh\left(\frac{W_B - x_{i+1}}{L_D}\right)}{L_D \cosh\left(\frac{x_{i+1} - x_i}{L_D}\right)} \cdot \left\{ \coth\left(\frac{x_{i+1} - x_i}{L_D}\right) + \tanh\left(\frac{x_i}{L_D}\right) \right\} \right] \\ & - \sum_{i=1}^n \left[\frac{N_{VS_{i+1}} q D_n}{L_D} \cdot \left\{ \frac{\cosh\left(\frac{W_B - x_{i+1}}{L_D}\right)}{\sinh\left(\frac{x_{i+1} - x_i}{L_D}\right) \cdot \cosh\left(\frac{x_{i+1} - x_i}{L_D}\right)} - \sinh\left(\frac{W_B - x_{i+1}}{L_D}\right) \right. \right. \\ & \quad \left. \left. + \tanh\left(\frac{x_{i+1} - x_i}{L_D}\right) \cosh\left(\frac{W_B - x_{i+1}}{L_D}\right) \right\} \right] \\ & + \sum_{i=1}^n J_{VS_{i+1}} \cosh\left(\frac{W_B - x_{i+1}}{L_D}\right) \end{aligned} \quad (4)$$

where the virtual current density over any n th QW at position x_n is expressed as

$$J_{VS_{n-1}} = J_{VS_n} \cosh\left(\frac{x_n - x_{n-1}}{L_D}\right) + \frac{q D_n N_{VS_n}}{L_D} \times \left[\sinh\left(\frac{x_n - x_{n-1}}{L_D}\right) + \coth\left(\frac{W_B - x_n}{L_D}\right) \cosh\left(\frac{x_n - x_{n-1}}{L_D}\right) \right]. \quad (5)$$

The base current is obtained from the conventional rule, $J_B = J_E - J_C$.

The connections between the carrier densities and current densities related to the QW and the VS are made through the relations [8]:

$$\frac{J_{VS}}{qd} = \frac{J_{QW}}{qd} - \frac{N_{VS}}{\tau_S} \quad \text{and} \quad \frac{J_{QW}}{qd} = \frac{N_{VS}}{\tau_{cap}} - \frac{N_{QW}}{\tau_{esc}}. \quad (6)$$

In above, τ_S , τ_{cap} , and τ_{esc} denote, respectively, the spontaneous recombination lifetime, capture time of electrons into the QW, and the escape time of electrons from the QW to the VS.

The expressions for terminal current densities given above reduce to the corresponding expressions for SQW given in ref. [10] by putting $n = 1$.

The insertion of $\text{In}_{1-x}\text{Ga}_x\text{As}$ QWs in the undoped GaAs base leads to strain in the QWs. The complete strain effect and the values for $E_{C, str}$ and $E_{V, str}$ are given in [10]. Gain characteristics are estimated by using (1) due to Asryan *et al.* [11], which is too lengthy to reproduce here.

The usual characteristics of a semiconductor laser is described by the coupled rate equations of carrier and photon, respectively, as [26]

$$\frac{dN}{dt} = \frac{I_B(t)}{q} - AS - \frac{N}{\tau} \quad (7)$$

$$\frac{dS}{dt} = (G - G_{th})S + \frac{C}{\tau_B} N \quad (8)$$

where A is the coefficient for linear gain, and C , the spontaneous emission factor, is defined by [26], $C = (a\Gamma\tau_B/V)$.

In above, a is the differential gain constant, which is calculated from first principle using the Fermi Golden rule and density-of-states function of the active medium, rather than taking it as a fitting parameter, and Γ is the confinement factor in the active layer volume V .

The stimulated emission provides another recombination channel in the QW. The overall effect is estimated by an effective lifetime defined as follows [25]

$$\tau^{-1} = \tau_B^{-1} + \Gamma v_g g N S \quad (9)$$

where τ_B is the base recombination lifetime, and the second term in τ represents the stimulated recombination lifetime. $S = \eta(I_B - I_{Bth}) / (q \cdot v_g \cdot \alpha_m)$ is the photon number per unit area. Here, η is the internal quantum efficiency, v_g is the group velocity, and α_m is the mirror loss. I_B is the usual base drive responsible for laser emission from active QW region (s).

Faster radiative lifetime results in small-signal perturbation in (7) and (8). In the small-signal analysis, a small sinusoidal perturbation in the base current is given around the modulating frequency f_m as

$$I_B(t) = I_b + I_m \cos(2\pi f_m t) = I_b + \left(\frac{I_m}{2} e^{2\pi j f_m t} + c.c. \right) \quad (10)$$

where I_b is the bias component or DC term, I_m is the modulating component, and $c.c.$ denotes complex conjugate. Separating the bias and modulation terms of (7) and (8), we are able to obtain the bias term for linear gain as, $A_b = (a\Gamma/V)(N_b - N_{tr})$ and the damping rates of carrier and photon concentrations, respectively, as

$$\Gamma_S = BS_b + \frac{C \cdot N_b}{S_b \tau_S} \quad \text{and} \quad \Gamma_N = \frac{a\Gamma}{V} S_b + \frac{1}{\tau} \quad (11)$$

where N_b and S_b are the bias components of carrier and photon concentration, and B is defined as the coefficient for nonlinear gain or gain suppression. Consequently, the confinement factors for different structures are also estimated from the calculated differential gain constant. The relaxation circular frequency defined as, with f_r as the relaxation oscillation frequency [26]

$$\Omega_r^2 = (2\pi f_r)^2 = \frac{a\Gamma}{V} \{S_b + 1\} A_b + \Gamma_N \Gamma_S. \quad (12)$$

The modulation performance of a TL is evaluated in terms of the transfer function from current modulation to optical power output for specific base bias currents. Thus, the modulation response becomes

$$\left| \frac{S_m(f_m)}{S_m(0)} \right|^2 = |H(f_m)| = \left\{ 1 + 2j \frac{f_m \Gamma_r}{f_r^2} - \left(\frac{f_m}{f_r} \right)^2 \right\}^{-1}. \quad (13)$$

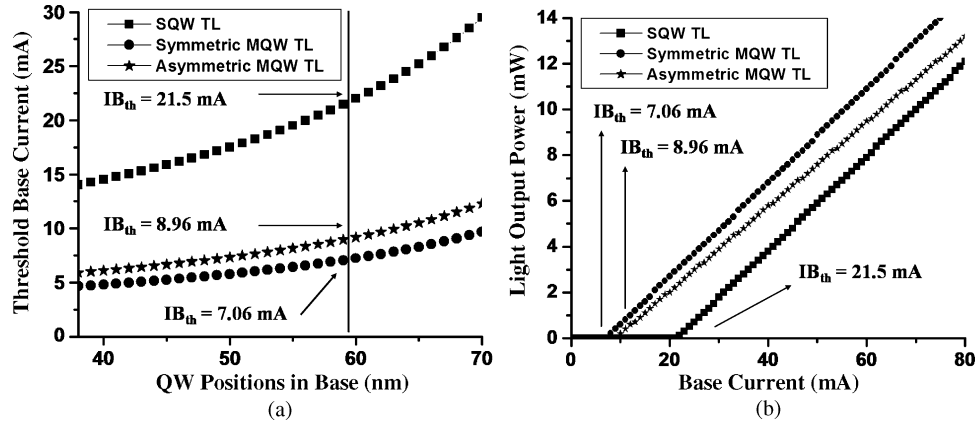


Fig. 2. (a) Variation of threshold base currents with QW positions across the base for SQW, S-MQW TL, and A-MQW TL structures. (b) Variation of light output power for different base current for SQW, S-MQW, and A-MQW TL structures.

At a specific bias current I_b or bias current density J_b , the modulation response H_m at a given frequency $\omega_m = 2\pi f_m$ is defined as the ratio of modulated photon number $s(\omega)$ to the corresponding unmodulated value $s(0)$. The modulation BW, i.e., the 3-dB frequency is defined as the value of frequency at which the response drops to one half of its value, and it is given as

$$f_{3dB} = \frac{1}{2\pi} \sqrt{(f_r^2 - 2\Gamma_r^2) + 2\sqrt{(f_r^2 - 2\Gamma_r^2)^2 + f_r^2\Gamma_r^2}} \quad (14)$$

where the damping factor $\Gamma_r = \tau^{-1}$ as in (9).

3. Results and Discussion

The parameters used for calculation are as follows: $T = 288K$, $W_B = 89$ nm, $\tau_{in} = 0.1$ ps, $\tau_B = 200$ ps, $\tau_{Cap} = 10$ ps, $\tau_{esc} = 5$ ns, $\tau_S = 15$ ns, $N_a = 3.5$; $C = 2.5 \times 10^{-5}$; $R_1 = R_2 = 32\%$; $\alpha = 500$ m $^{-1}$; $\tau_P = 8.8$ ps; $v_g = 6.67 \times 10^7$ m/sec. The values of parameters for alloys, such as their mass, permittivity, etc., are calculated by linear interpolation of the data [10].

The initial VS carrier density at first QW is given as input (taken as quite larger than transparency). The VS carrier density for other two QWs are estimated by the QW geometry factor that gives the fraction of base charge captured in QW as, $\gamma_1 = (d/W_B)(1 - (x_{QW1}/W_B))$. Thus, VS carrier density over QW2 is estimated as, $N_{VS2} = N_{VS1}(1 - \gamma_1)$. Similarly, $N_{VS3} = N_{VS2}(1 - \gamma_2)$ is evaluated. Here, x_{QWi} is the position of the i th QW.

The gain in the QW is obtained by considering subband energies and envelope functions in the presence of strain, 2-D density-of-states function, polarization-dependent momentum matrix element, Fermi distribution function, Fermi Golden rule, and lineshape function [10], [11].

In the symmetric case, the three QWs, each of width 16 nm, are assumed to be placed at $x_1 = 39$ nm, $x_2 = 59$ nm, and $x_3 = 79$ nm across the base. We have used as the basis of comparison the value of 21.5 mA for base threshold current and light power output for a strained InGaAs SQW placed at 59 nm in GaAs base of width $W_B = 88$ nm [10]. For an S-MQW structure, the calculated threshold base current is 7.06 mA with the middle QW placed at 59 nm; this value is substantially lower than the value of 21.5 mA for SQW TL. The light power output for SQW did agree with the experimental values [3], keeping in view the uncertainty in laser-fiber coupling loss. As expected, higher values of light power and lower values of base thresholds are indeed obtained for both the S-MQW and A-MQW TL structures (see Fig. 2). In asymmetric structure, base threshold currents for the QWs placed at 39 nm (width of 12 nm), 59 nm (width of 16 nm), and 79 nm (width of 18 nm) positions are 7.81, 8.96, and 15.82 mA, respectively. It appears that there is a slight

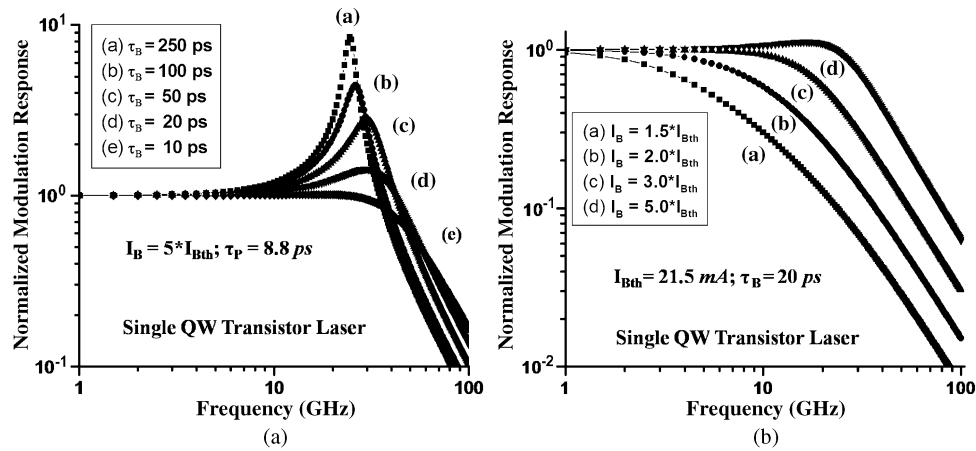


Fig. 3. (a) Calculated optical response function for SQW TL structure for various values of base emission lifetime. (b) Calculated optical response with increasing biases for SQW TL structure with the middle QW placed at 59 nm. A small bump in response is observed for higher bias.

increase in base threshold current in the A-MQW TL structure than in the SQW TL structure. The confinement factors for the three QWs are calculated as 1.89%, 10.64%, and 11.82%, respectively.

Fig. 2(a) shows the plot of threshold base current variation with the middle QW positioned at different points in the base and with equal barrier width of 20 nm. The calculated values of light output power for different base currents are shown in Fig. 2(b). Here also, we made comparison for SQW, S-MQW, and A-MQW structures. The calculated power output P increases linearly with base current according to the relation [10], $P = (\hbar\omega/q)[\alpha_m/(\alpha_m + \alpha_i)][I_B - I_{Bth}]$, where α_m denotes mirror loss. As usual, the output power increases sharply once the threshold base current for the QWs are reached. The reduction in the base threshold current is largest for S-MQW TL, and at the same time, the rate of rise of output power is highest in this case, as is evident from Fig. 2.

We have studied the small-signal modulation response and made a comparison of 3-dB modulation BWs of all the aforementioned structures at three bias points. For $I_B/I_{Bth} = 3$, modulation BWs are 21, 25, and 28 GHz, respectively, for SQW, S-MQW, and A-MQW TL structures. Similarly, for $I_B/I_{Bth} = 5$, the values are 31, 35, and 58 GHz.

Fig. 3(a) shows the variation of optical response for different base recombination lifetimes in an SQW TL. Here, gain and other quantities are calculated following [10] instead of taking the gain constant, etc., as fitting parameters [6]. As the recombination time τ_B varies from 250 to 10 ps, the peak is eliminated gradually from the response due to gradual decrease in carrier–photon interactions. The usual resonance peaks appear for larger emission lifetimes, but as the lifetime is as low as 10 ps, the peak disappears; as a result, modulation BW, in turn, increases gradually. With the faster recombination lifetime, the resonance peak makes a red shift also. In fact, the resonance-free operation is obtained for lifetime of about 17–18 ps for SQW TL structure, which is close to the experimental value of 29 ps obtained in [6], and 23–27 ps for spontaneous heterojunction bipolar light-emitting transistor [6] with photon lifetime and bias current set to $\tau_P = 8.8$ ps and $I_B/I_{Bth} = 5$, respectively, for all cases. It is to be noticed that around $\tau_B \sim 10$ ps, the response starts to show the critically damped conditions.

Fig. 3(b) shows how the resonance-free modulation BW increases as we gradually increase the bias current from its threshold value for the SQW TL. The threshold base current is set at 21.5 mA, as found in [10]. We fix the value of lifetime to 20 ps, since around 17–18 ps, the damping starts completely in the structure, and study how the resonance-free response is related to the increase in normalized base current. It is found that damped response may occur even under a lower base current, which is quite unusual in the ordinary laser diode case. The resonance of small magnitude observed at higher bias may be due to higher carrier depletion even at the presence of faster recombination.

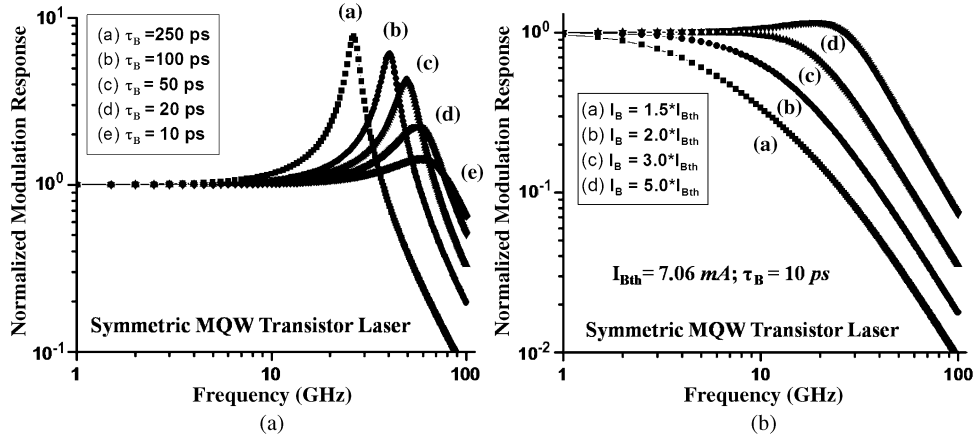


Fig. 4. (a) Calculated optical response function for S-MQW TL structure for various values of base emission lifetime. (b) Calculated optical response with increasing biases for S-MQW TL structure with the middle QW placed at 59 nm. A small bump in response is observed for higher bias.

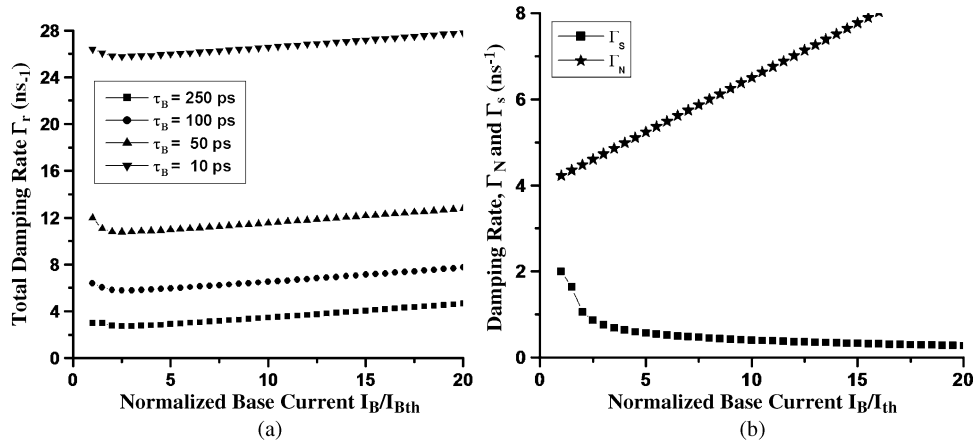


Fig. 5. (a) Variation of overall damping rate for an SQW TL with normalized base current for various base emission lifetimes as parameter. (b) Variation of damping rate components of carrier and photon concentration with normalized base current.

Fig. 4 shows the optical responses of S-MQW TLs. Different curves in Fig. 4(a) show the response for different lifetimes for a fixed normalized bias $I_B/I_{Bth} = 5$, and curves in Fig. 4(b) depict the response with bias currents as parameter with $\tau_P = 8.8$ ps. The complete damping occurs for τ_B below 10 ps. The response curves for A-MQWs are similar to the curves in Figs. 3 and 4 and are not shown here. The values of BW for $I_B/I_{Bth} = 3(5)$ are 21(31), 25(25), and 28(58) GHz for SQW, S-MQW, and A-MQW, respectively. The damping is found to occur below 10 ps, while some resonance is still observed even at 10 ps in symmetric structure. For faster base recombination lifetime, less damping rate results in less ringing, i.e., resonance-free responses in comparison to ordinary laser diodes where spontaneous lifetime ~ 1 ns causes ringing at very large biases and incorporation of low-pass filters complicates the receiver circuitry.

Fig. 5(a) plots the variation of damping rates against normalized bias current for different base recombination lifetimes. For the same base current, a faster base recombination lifetime leads to higher damping rate according to (12) and reduces the height of resonance peak. With τ_B reaching 10 ps, the damping rate increases drastically, and all the structures show a critically damped condition. Fig. 5(b) shows how the damping rate components of carrier and photon concentrations vary individually with normalized base current.

The present model shows that a reduction in threshold current and an enhancement of modulation BW and even resonance-free modulation characteristics may be obtained for MQW TLs. However, there are practical problems in the fabrication, which are discussed in detail by Duan *et al.* [27].

4. Conclusion

We have incorporated three QWs in the base of an InGaP–GaAs–GaAs HBT laser and studied how the threshold base current and light power output change from the corresponding calculated values for a TL with an SQW in the base. The calculated values for SQW TL were found to agree with experimental values. The MQWs are assumed to have equal widths (symmetric) as well as to have different widths placed at different positions in the base. In general, lower threshold base current and higher light power outputs are obtained for MQW TLs in comparison to the corresponding values calculated for SQW TLs. It is also found that faster recombination lifetime above threshold due to onset of the stimulated process leads to resonance ringing-free modulation response, which is advantageous for high-bit-rate optical communication even at lower base biases.

References

- [1] N. Holonyak, Jr. and M. Feng, "The transistor laser," *IEEE Spectr.*, vol. 43, no. 2, pp. 50–55, Feb. 2006.
- [2] M. Feng, N. Holonyak, Jr., and W. Hafez, "Light-emitting transistor: Light emission from InGaP/GaAs heterojunction bipolar transistors," *Appl. Phys. Lett.*, vol. 84, no. 1, pp. 151–153, Jan. 2004.
- [3] G. Walter, N. Holonyak, Jr., M. Feng, and R. Chan, "Laser operation of a heterojunction bipolar light-emitting transistor," *Appl. Phys. Lett.*, vol. 85, no. 20, pp. 4768–4770, Nov. 2004.
- [4] M. Feng, N. Holonyak, Jr., A. James, K. Cimino, G. Walter, and R. Chan, "Carrier lifetime and modulation bandwidth of a quantum well AlGaAs/InGaP/GaAs/InGaAs transistor laser," *Appl. Phys. Lett.*, vol. 89, no. 11, pp. 131504-1–131504-3, Sep. 2006.
- [5] M. Feng, N. Holonyak, Jr., H. W. Then, and G. Walter, "Charge control analysis of transistor laser operation," *Appl. Phys. Lett.*, vol. 91, no. 5, pp. 053501-1–053501-3, Jul. 2007.
- [6] M. Feng, H. W. Then, N. Holonyak, Jr., G. Walter, and A. James, "Resonance-free frequency response of a semiconductor laser," *Appl. Phys. Lett.*, vol. 95, no. 3, pp. 033509-1–033509-3, Jul. 2009.
- [7] H. W. Then, M. Feng, and N. Holonyak, Jr., "Microwave circuit model of the three-port transistor laser," *J. Appl. Phys.*, vol. 107, no. 9, pp. 094509-1–094509-7, May 2010.
- [8] B. Faraji, W. Shi, D. L. Pulfrey, and L. Chrostowski, "Analytical modeling of the transistor laser," *IEEE J. Sel. Topics Quantum Electron.*, vol. 15, no. 3, pp. 594–603, May/Jun. 2009.
- [9] L. Zhang and J. P. Leburton, "Modeling of the transient characteristics of heterojunction bipolar transistor lasers," *IEEE J. Quantum Electron.*, vol. 45, no. 4, pp. 359–366, Apr. 2009.
- [10] R. Basu, B. Mukhopadhyay, and P. K. Basu, "Estimated threshold base current and light power output of a transistor laser with InGaAs quantum well in GaAs base," *Semicond. Sci. Technol.*, vol. 26, no. 10, pp. 105014-1–105014-6, Oct. 2011.
- [11] L. V. Asryan, N. A. Gun'ko, A. S. Polkivnikov, G. G. Zegrya, R. A. Suris, P. K. Lau, and T. Makino, "Threshold characteristics of InGaAsP/InP multiple quantum well lasers," *Semicond. Sci. Technol.*, vol. 15, no. 12, pp. 1131–1140, Dec. 2000.
- [12] I. Taghavi, H. Kaatuzian, and J. P. Leburton, "Bandwidth enhancement and optical performances of multiple quantum well transistor lasers," *Appl. Phys. Lett.*, vol. 100, no. 23, pp. 231114-1–231114-5, Jun. 2012.
- [13] B. Faraji, D. L. Pulfrey, and L. Chrostowski, "Small-signal modelling of the transistor laser including the quantum capture and escape lifetimes," *Appl. Phys. Lett.*, vol. 93, no. 10, pp. 103509-1–103509-3, Sep. 2008.
- [14] M. Shirao, S. Lee, N. Nishiyama, and S. Arai, "Large signal analysis of a transistor laser," *IEEE J. Quantum Electron.*, vol. 47, no. 3, pp. 359–367, Mar. 2011.
- [15] N. Tansu and L. J. Mawst, "Current injection efficiency of InGaAsN quantum-well lasers," *J. Appl. Phys.*, vol. 97, no. 5, pp. 054502-1–054502-18, Mar. 2005.
- [16] R. Nagarajan, M. Ishikawa, T. Fukushima, R. S. Geels, and J. E. Bowers, "High speed Quantum Well Lasers and carrier transport effects," *IEEE J. Quantum Electron.*, vol. 28, no. 10, pp. 1990–2008, Oct. 1992.
- [17] R. Nagarajan and J. E. Bowers, "Effects of carrier transport on injection efficiency and wavelength chirping in quantum-well lasers," *IEEE J. Quantum Electron.*, vol. 29, no. 6, pp. 1601–1608, Jun. 1993.
- [18] N. Tansu and L. J. Mawst, "The role of hole leakage in 1300-nm InGaAsN quantum-well lasers," *Appl. Phys. Lett.*, vol. 82, no. 10, pp. 1500–1502, Mar. 2003.
- [19] N. Tansu, J.-Y. Yeh, and L. J. Mawst, "Experimental evidence of carrier leakage in InGaAsN quantum-well lasers," *Appl. Phys. Lett.*, vol. 83, no. 11, pp. 2112–2114, Sep. 2003.
- [20] A. Albo, G. Bahir, and D. Fekete, "Improved hole confinement in GaInAsN–GaAsSbN thin double-layer quantum-well structure for telecom-wavelength lasers," *J. Appl. Phys.*, vol. 108, no. 9, pp. 093116-1–093116-6, Nov. 2010.
- [21] Q. Wei, J. S. Gustavsson, Å. Haglund, P. Modh, M. Sadeghi, S. M. Wang, and A. Larsson, "High-frequency modulation and bandwidth limitations of GaInNAs double quantum-well lasers," *Appl. Phys. Lett.*, vol. 88, no. 5, pp. 051103-1–051103-3, Jan. 2006.

- [22] O. Anton, L. F. Xu, D. Patel, C. S. Menoni, J. Y. Yeh, T. T. Van Roy, L. J. Mawst, and N. Tansu, "The Intrinsic Frequency Response of 1.3- μm InGaAsN Lasers in the Range $T = 10\text{ }^{\circ}\text{C}$ – $80\text{ }^{\circ}\text{C}$," *IEEE Photon. Technol. Lett.*, vol. 18, no. 16, pp. 1774–1776, Aug. 2006.
- [23] H. Zhao, G. Liu, R. A. Arif, and N. Tansu, "Current injection efficiency induced efficiency-droop in InGaN quantum well light-emitting diodes," *Solid State Electron.*, vol. 54, no. 10, pp. 1119–1124, Oct. 2010.
- [24] T.-S. Kim, B.-J. Ahn, Y. Dong, K.-N. Park, J.-G. Lee, Y. Moon, H.-K. Yuh, S.-C. Choi, J.-H. Lee, S.-K. Hong, and J.-H. Song, "Well-to-well non-uniformity in InGaN/GaN multiple quantum wells characterized by capacitance–voltage measurement with additional laser illumination," *Appl. Phys. Lett.*, vol. 100, no. 7, pp. 071910-1–071910-4, Feb. 2012.
- [25] R. Basu, B. Mukhopadhyay, and P. K. Basu, "Modeling of current gain compression in common emitter mode of a transistor laser above threshold base current," *J. Appl. Phys.*, vol. 111, no. 8, pp. 083103-1–083103-7, Apr. 2012.
- [26] M. Ahmed and A. El-Lafi, "Analysis of small-signal intensity modulation of semiconductor lasers taking account of gain suppression," *Pramana*, vol. 71, no. 1, pp. 99–115, Jul. 2008.
- [27] Z. Duan, W. Shi, L. Chrostowsky, X. Huang, N. Zhou, and G. Chai, "Design and epitaxy of 1.5 μm InGaAsP–InP MQW material for a Transistor Laser," *Opt. Exp.*, vol. 18, no. 2, pp. 1501–1509, Jan. 2010.